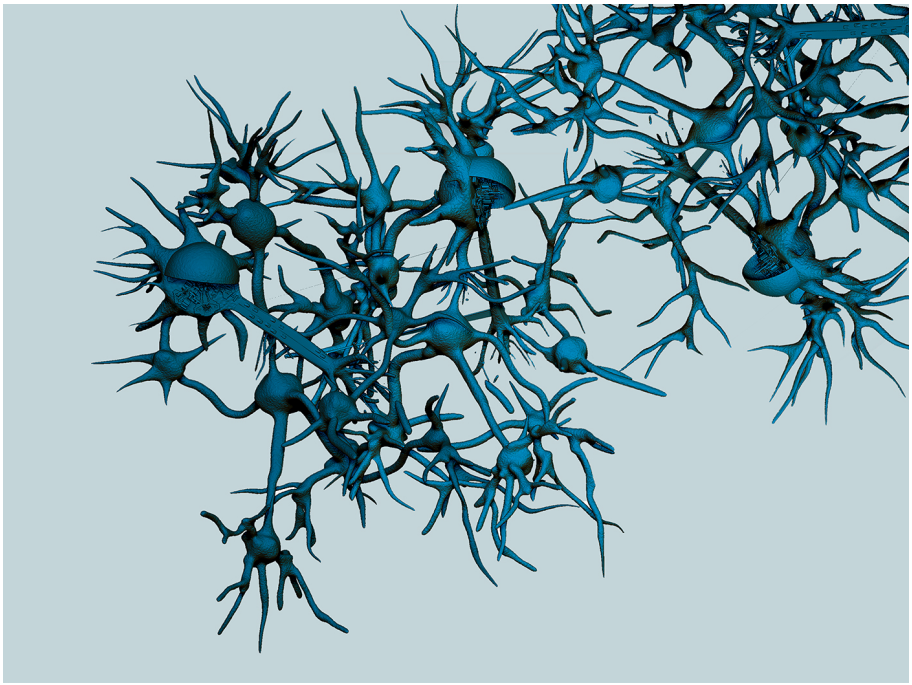

Spiking neural networks:
Optimization of the Izhikevich neuron

Optimization of the Izhikevich neuron using evolutionary algorithms to maximize spike coincidence to measured data

Bachlor's thesis in Engineering Mathematics

Peter Svenningsson

Mechanics and Maritime Sciences
CHALMERS UNIVERSITY OF TECHNOLOGY
Gothenburg, Sweden 2021

Spiking neural networks: optimization of the Izhikevich neuron
Optimization of the Izhikevich neuron using evolutionary algorithms to maximize spike coincidence to measured data
Peter Svenningsson
Mechanics and Maritime Sciences
Chalmers University of Technology

Abstract

This work aims to fit dynamical models of single neurons to data measured in-vitro. The dataset consists of measurements of a regular spiking pyramidal cell stimulated by in-vivo-like current. The neural models are fit to the dataset using genetic algorithms with a fitness function based on a comparison of the spiking events generated by the model and observed in the dataset.

The single neuron models evaluated in this work are variations of the Izhikevich neuron and the leaky integrate-and-fire (LIF) model. Variations of the Izhikevich neuron comprises the addition of second degree polynomials to the dynamical model as well as the addition of a resistance factor to the input current.

The top performing Izhikevich model achieved a match distance score of 99.84% on unseen data. The more simple LIF model performed competitively with a match distance score of 99.72%. Therefore, it is argued that a one dimensional dynamical system is sufficient to model the spiking activity of a regular spiking neuron. Moreover, the results indicate that the two-dimensional Izhikevich model generate spiking profiles more similar to those observed in the measured data in comparison to spiking profiles generated by the LIF model.

Contents

1 Introduction

In 1952 Hodgkin and Huxley [1] proposed a mathematical model for the behavior of a giant squid axon. This work included uncovering the ionic mechanism of action potentials which awarded the pair the Nobel Prize in physiology or medicine in 1963. The model proposed by Hodkin and Huxley is composed of four differential equations with tens of parameters which is able to reproduce a large set of neuron firing behavior. However, the large parameter search space and the computational expense of the model has prevented its use in computational neuroscience [2].

A large number of dynamical models have been created to capture the behavior of single neurons. The complexity of the models is generally classified by the number of tunable parameters and the dimensionality of the dynamical system. A well established one-dimensional model for the membrane voltage v is the leaky integrate-and-fire model

$$v' = I + a - bv, \text{ if } v \geq v_{\text{peak}} \text{ , then v } \leftarrow c, \tag{1}$$

which is computationally efficient to evaluate but is only able to reproduce a limited number of neural firing patterns [2]. A review of common dynamic models [3] provides further insight into the diverse field of single neuron models.

A two dimensional model for cortical neurons was proposed by Izhikevich [4] in a simple parametrized form

$$\begin{aligned} v' &= 0.04v^2 + 5v + 140 - u + I \\ u' &= a(bv - u) \\ \text{if } v \geq 30\text{mV, then } &\begin{cases} v \leftarrow c \\ u \leftarrow u + d \end{cases}, \end{aligned} \tag{2}$$

and in an extended parametrized form

$$\begin{aligned} C\dot{v} &= k\left(v - v_{\text{r}}\right)\left(v - v_{\text{t}}\right) - u + I \\ \dot{u} &= a\left\{b\left(v - v_{\text{r}}\right) - u\right\} \\ \text{if } v \geq v_{\text{peak}} \text{ , then } &\begin{cases} v \leftarrow c \\ u \leftarrow u + d \end{cases}. \end{aligned} \tag{3}$$

These models are able to reproduce the same set of neuron firing behaviour as the Hodgkin-Huxley neuron while being less computationally expensive to evaluate. The computational efficiency of the Izhikevich neuron has made possible novel research such as numerical studies into the computational and memory capacity of excitatory and inhibitory neurons [5].

The development of valid and computationally feasible models of neurons is important for a number of practical applications such as brain-computer interfaces (BCI). Recently, some research has been done in neuroprosthetics focusing on using Izhikevich neuron model to formulate control problems for the actuation of robotic components [6]. This application naturally relies on the efficacy of the neural model and the ability to evaluate it in real time. Validation studies of the Izhikevich neuron are therefore of interest.

It is of particular importance to validate the Izhikevich neuron model for in-vivo-like current input, current input which mimics the conditions inside a living organism. Classification of neurons is commonly based on the neuron's amplitude response to a current step signal. Izhikevich [4] validated that his model is able to reproduce a large selection of neuron classifications. However, it has been shown that a neuron responds highly reliably to repeated injections of in-vivo-like current input while the response for a current step signal vary widely across trials [7], [8]. For purposes of validating the

predictive power of a model it is therefore meaningful to evaluate the model on measurements from in-vivo-like current input.

1.1 Previous work

The International Neuroinformatics Coordinating Facility (INCF) held the Quantitative Single Neuron Modeling Competition in 2008 and in 2009 with the aim to evaluate the predictive strength of single neuron models [9], [10]. A dataset consisting of measurements of a pyramidal neuron stimulated by an in-vivo like current has been publicly released by INCF [11].

Previous work has explored fitting the simple parameterization of the Izhikevich neuron (2) to the dataset [11] using evolutionary algorithms with the van Rossum similarity metric as a fitness function [12] or the coincidence rate as a fitness function [13], achieving comparable results. The simple Izhikevich neuron has also been fit to experimental data using the inverse of the residual as the fitness function [14]. Classical optimization algorithms such as the interior-point has also been explored for fitting the parameters of the simple Izhikevich neuron [15].

1.2 Aim

The aim of this study is to fit the extended and simplified parametrizations of the Izhikevich neuron to the QSNMC dataset [11] which consists of measurements of a single neuron stimulated by in-vivo-like current injection. The predictive strength of the models will be evaluated by validating the model on a portion of the dataset not used to fit the model. Furthermore, structural changes to the extended parametrization (3) will be evaluated.

1.3 Limitations

The dataset consists of 21 s of recorded data of a pyramidal neuron stimulated by in-vivo-like current injection. The dataset is too small for a training, validation and test set split, commonly referred to as holdout validation [16]. Instead, the dataset is split into a training and validation set. Therefore, model choices such as structural changes or the selection of parameter intervals may lead to some overfitting to the validation dataset.

In the exploration of structural changes to the Izhikevich neuron only the addition of second degree polynomials are evaluated. This restriction is mainly to limit the computational resources needed.

2 Theory

Information presented here covers theory of dynamical systems necessary to derive the Izhikevich neuron from the Hodkin-Huxley model. A overview of the Hodkin-Huxley is presented as well as similarity measures to evaluate the efficacy of single neuron models. Lastly, a overview of genetic algorithms is also covered.

2.1 Dynamical systems

A dynamical system is a set of equations which describes the change of state variables $\mathbf{x} = [x_1, \ldots, x_n]^T$ over time. The dynamical models discussed in this study are systems of autonomous nonlinear ordinary differential equations on the form

$$\dot{\mathbf{x}} = f(\mathbf{x}, \theta), \tag{4}$$

where f is a vector valued function and θ denotes the parameters of the model.

A solution to (4) expressed as $x_2 = g(x_1)$ is named a trajectory of (4). For $n = 2$ the behavior of (4) can be visualized as a phase portrait, a plot of several trajectories of the system. Solutions to initial value problems for linear ordinary differential equations are unique [17]. It follows that the trajectories may not cross each other and therefore the phase portrait provides an interpretable illustration of the dynamical system.

A nullcline of (4) is a curve along $\dot{x}_i = 0$. The nullclines of a two dimensional system may be plotted in the phase portrait to illustrate the signs of $\dot{\mathbf{x}}$ in different areas of the phase portrait. The intersection of the nullclines of a system is by definition a stationary point.

The dynamics of (4) depend on the model parameter θ. Assume that (4) has one stable equilibrium point at θ_1 and one unstable equilibrium point at θ_2. The value for θ where the system transitions from having a stable to an unstable equilibrium point is named a bifurcation point and signifies a qualitative change in the dynamic of the system.

2.2 Spike trains

Neurons generate spikes through sudden changes in membrane voltage. These processes are controlled by various ion channels in the cell membrane. A spike is formed when the voltage quickly rises to a high value and shortly thereafter falls back into a typical range. A sequence of recorded spiking events is referred to as a spike train. One can consider a spike train as a time series S of spiking events s_i

$$S = \{s_1, s_2, \ldots, s_n\}, s_1 < s_2 < \cdots < s_n, \tag{5}$$

generated by a unknown dynamical system for the membrane voltage.

However, repeated trials of recording spike trains indicate that the generation and recording of spike trains is not a deterministic process [7]. Therefore one can more formally describe the set in equation (5) as realizations of a point process. For the purposes of this study a point process is defined as a random set $\mathbb{S} = \{s_i\}_{i=1}^N$ with the firing intensity $v = \mathbb{E}[S]$, avoiding a more complex description.

The spiking times of a neuron are highly dependent on previous spiking times. For instance, after a spike event there exists a refractory period during no new spikes can occur. It follows that the point process $\mathbb{S}$ is not memory-less and cannot be modelled as a Poisson process.

A common representation of spike trains is the inter-spike intervals (ISIs) $X = \{x \mid x_i = s_i - s_{i-1}\}$ which denotes the elapsed time between two subsequent spiking events. The ISIs can also be considered as realizations of some point process.

2.2.1 All-or-none principle

The all-or-none principle proposes that the peak membrane voltage of the neuron's action potential spike is independent of the size of the input current and roughly constant. This principal seems to be supported empirically [18]. There is some support for the notion that information is therefore encoded in the ISIs patterns produced by the neurons which would justify the representation of the neurons' output as a time series of spiking events [19].

2.3 Electrophysiology of neurons

A neuron is composed of a main cell body, dendrites and an axon. The dendrites connects the neuron cell to the axons of other neurons and allows for ionic compounds to travel through the cell membrane from the connected neurons to the cell body. The difference in concentration of ionic compounds inside the cell and in the medium outside the cell generates an electric potential over the cell membrane [18].

Electric current in neurons is propagated by ions passing through the cell membrane. The ionic compounds are sodium Na^+, potassium K^+, calcium Ca^{2+}, chloride Cl^- and large negatively charged molecules here denoted A^-. The medium inside the cell membrane has a high concentration of A^- ions which cannot pass through the cell membrane. Therefore at equilibrium there exists concentration gradients which are canceled out by electric potential gradients. [20].

The ionic compounds pass through the membrane in gated channels which consists of large protein molecules facilitating the passing of one or several of the ionic compounds. The channel is classified as passive if the compounds pass based on the concentration gradient and the electric potential gradient between the medium inside the cell and the outside medium. In contrast, an active channel transports ions at a fixed ratio. For example, a Na^+-K^+ active channel removes three Na^+ from the cell for every two K^+ ions pumped into the cell [20].

When a channel is inactive no ionic compound is passed through that channel. Channels may be activated by the cell's membrane potential, the concentration level of the ionic compounds, by neurotransmitters such as kainic acid or a combination of these factors [20].

The conductance of an ionic compound is determined by the collective behavior of the membrane channels and is therefore dependent on the membrane voltage. Action potentials are generated as an input signal increases the membrane potential past some threshold which increases the conductance of a positive ion compound such as K^+. The increased flow of the positive ion quickly increases the membrane potential until a peak threshold has been reached which releases positive ions from the cell and lets negative ions into the cell, rapidly decreasing the membrane potential [20].

2.4 Modeling Neurons as dynamical systems

The Hodgkin-Huxley model [1] models the membrane potential V from three ionic currents for the compounds K^+, Na^+ and Cl^-. The dynamical model

$$\begin{aligned} C\dot{V} &= I \overbrace{-\bar{g}_{\mathrm{K}} n^4 (V - E_{\mathrm{K}})}^{I_{\mathrm{K}}} \overbrace{-\bar{g}_{\mathrm{Na}} m^3 h (V - E_{\mathrm{Na}})}^{I_{\mathrm{Na}}} \overbrace{-g_{\mathrm{L}} (V - E_{\mathrm{L}})}^{I_{\mathrm{L}}} \\ \dot{n} &= \alpha_n(V)(1-n) - \beta_n(V)n \\ \dot{m} &= \alpha_m(V)(1-m) - \beta_m(V)m \\ \dot{h} &= \alpha_h(V)(1-h) - \beta_h(V)h, \end{aligned} \tag{6}$$

models the compound-specific currents I_{K} and I_{Na} as well as the leak current I_{L} which described a non-gated leak of ionic compounds mostly consisting of Cl^- ions [20]. C denotes the membrane capacitance and I denotes an externally applied current.

Observe the expression

$$I_{\mathrm{Na}} = \bar{g}_{\mathrm{Na}} m^3 h (V - E_{\mathrm{Na}}) \tag{7}$$

which models the Na^+ ionic current across the complete cell membrane. The maximum conductance $\bar{g}_{\mathrm{Na}}$ and the reverse potential E_{Na} are constant parameters in the model. The reverse potential E_{Na} is determined by the concentration gradient of Na^+ inside the cell and the outside medium which vary as ionic compounds are transported across the cell membrane. Therefore, the constant parameter E_{Na} is an approximation.

The Na^+ channels in (7) are modelled with three voltage dependent activation gates and one voltage dependent deactivation gate. The activation variable m is bounded to $[0, 1]$ and can be interpreted as the probability that a single activation gate is open. Similarly, the inactivation variable h can be interpreted as the probability that a single inactivation gate is open. Activation gates are likely to be open and inactivation gates tend to be closed when V is large, see Figure 1. The α and β functions are exponential functions fitted to experimental data. A squid axon can be approximated by the parameters [1]

$$\begin{aligned} \alpha_m(V) &= 0.1 \frac{25 - V}{\exp\left(\frac{25-V}{10}\right) - 1}, \quad \beta_m(V) = 4 \exp\left(\frac{-V}{18}\right), \\ \alpha_h(V) &= 0.07 \exp\left(\frac{-V}{20}\right), \quad \beta_h(V) = \frac{1}{\exp\left(\frac{30-V}{10}\right) + 1}, \\ E_{\mathrm{K}} &= -12\mathrm{mV}, \quad E_{\mathrm{Na}} = 120\mathrm{mV}, \quad E_{\mathrm{L}} = 10.6\mathrm{mV}, \\ \bar{g}_{\mathrm{K}} &= 36\mathrm{mS/cm^2}, \quad \bar{g}_{\mathrm{Na}} = 120\mathrm{mS/cm^2}, \quad g_{\mathrm{L}} = 0.3\mathrm{mS/cm^2}. \end{aligned} \tag{8}$$

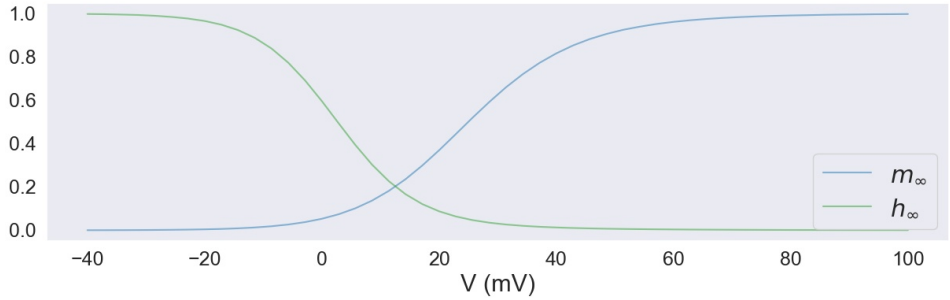

Figure 1: The asymptotic curves of m and h defined by parameters in (8) for varying V. Note that the deactivation gate variable h decreases as the membrane voltage V increases. In contrast, the activation gate variable m increases with V.

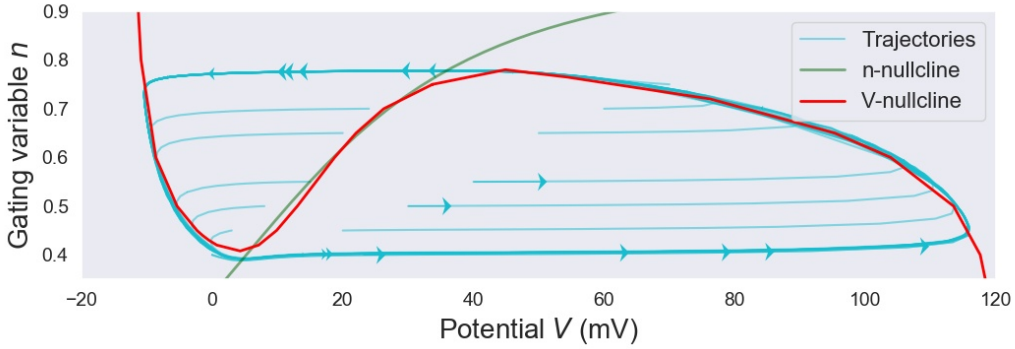

Figure 2: The nullclines of the dynamical system (9) plotted together with trajectories of the system for $I = 10$ mA.

The Hodgkin-Huxley model is capable of simulating an action potential. From a resting state, an increase in the membrane voltage will increase the activation variables m and n while decreasing the inactivation variable h. The dynamic of the activation variable m is fast relative to the two other gating variables and quickly increases the current I_{Na}. The increase of the membrane voltage will further increase the activation variable m which in turn causes a spike in the membrane voltage. After a short time the inactivation variable $h \to 0$ causing an inactivation of I_{Na}. At this time $n \to 1$ and the negative current I_K causes a decrease in V until the resting state has been reached. The slow dynamic of the h and n variables causes a refractory period after a spiking event. During the refractory period no spiking events can occur.

2.4.1 Reduction of the Hodgkin-Huxley model

The four dimensional Hodgkin-Huxley model in (6) can be reduced to a two dimensional model by introducing two approximations. The fast dynamics of the I_{Na} current can be approximated as instantaneous, $m = m_\infty(V)$. Krinskiĭ and Kokoz [21] discovered a second approximation, $n + h \approx 0.84$ by numerical analysis. The reduced Hodgkin-Huxley model is then described as

$$\begin{aligned} C\dot{V} &= I \overbrace{-\bar{g}_{\mathrm{K}} n^4 \left(V - E_{\mathrm{K}}\right)}^{I_{\mathrm{K}}} \overbrace{-\bar{g}_{\mathrm{Na}} m_\infty^3(V)(0.89 - n)\left(V - E_{\mathrm{Na}}\right)}^{I_{\mathrm{Na}}} \overbrace{-\bar{g}_{\mathrm{L}}\left(V - E_{\mathrm{L}}\right)}^{I_{\mathrm{L}}} \\ \dot{n} &= \left(n_\infty(V) - n\right)/\tau_n(V), \quad \tau_n = 1/\left(\alpha_n + \beta_n\right). \end{aligned} \tag{9}$$

The nullclines of the reduced model (9) can be calculated numerically and are visualized in Figure 2.

The input current I can be used as a bifurcation parameter by holding it constant for all t. For low input currents the system has one stable equilibrium which corresponds to the resting state of the neuron. For a sufficiently large I the dynamical system has a limit cycle attractor which corresponds to periodic spiking activity, see Figure 3. The transition from one stable equilibrium to a limit cycle attractor occurs at the bifurcation point I_0 which corresponds to the rheobase of the neuron, the lowest current amplitude for which the neuron produces spiking events.

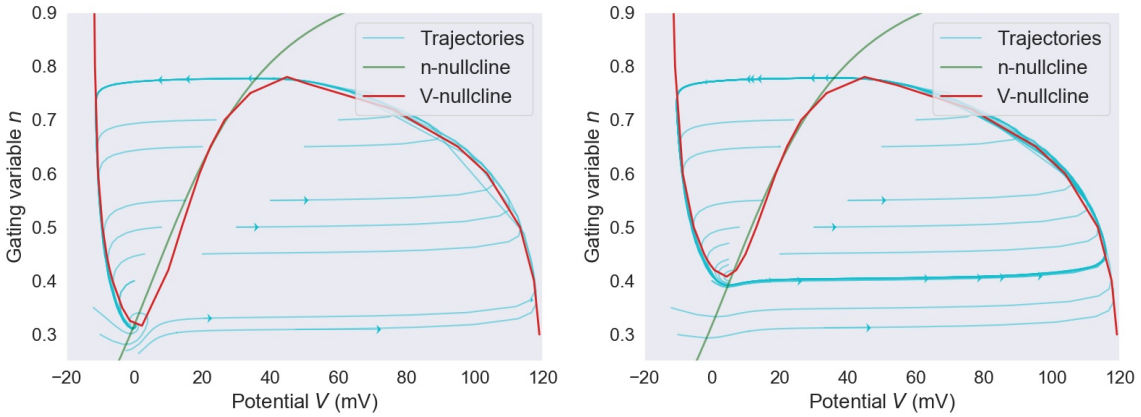

(a) A stable equilibrium, $I = 0$ mA. **(b)** A limit cycle attractor, $I = 10$ mA

Figure 3: The dynamics of (9) exhibiting a stable equilibrium and exhibiting a limit cycle attractor.

2.4.2 Derivation of the Izhikevich neuron

The Izhikevich neuron (3) approximates the geometry of the phase plane of (9) near the resting equilibrium, see Figure 4. As a result the model is able to reproduce the conditions needed for spiking events but is less able to reproduce the shape of the spike.

Close to the equilibrium as seen in Figure (4) the v-nullcline can be approximated by a quadratic parabola

$$n = n_{min} + a(v - v_{min})^2, \quad a > 0, \tag{10}$$

and the n-nullcline can be approximated as linear

$$n = b(v - v_r), \tag{11}$$

where v_r denotes the intercept on the along the v-axis.

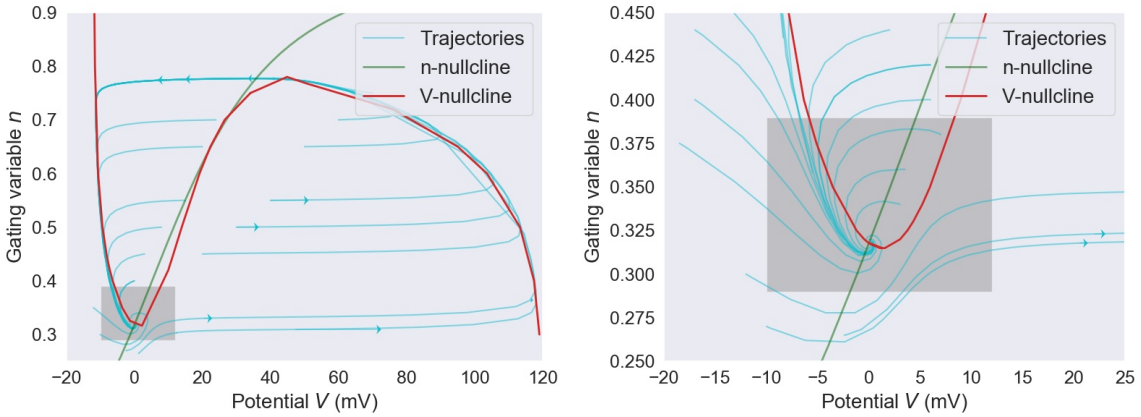

(a) A stable equilibrium, $I = 0$ mA. **(b)** Detailed view close to the equilibrium point.

Figure 4: A phase portrait of (9). The Izhikevich neuron approximates the dynamics of the shaded region close to the equilibrium point.

A dynamical system with the nullclines (10) and (11) can be constructed as

$$\begin{aligned} \dot{v} &= \tau_{\mathrm{f}} \left\{ p \left(v - v_{\min} \right)^2 - \left(n - n_{\min} \right) \right\} \\ \dot{n} &= \tau_{\mathrm{s}} \left\{ b \left(v - v_r \right) - n \right\} \end{aligned} \tag{12}$$

with τ_f and τ_s denoting the time scales of v and n. The update rule

$$\text{if } v \geq v_{\text{peak}} \text{ , then } \begin{cases} v \leftarrow c \\ n = n + d \end{cases} \tag{13}$$

is added to mimic the behavior of the orbits which leaves the shaded region in Figure 4 from the right and re-enters the shaded region from the left. The form of (12) with update rule (13) is then equivalent to the Izhikevich neuron (3).

2.5 Similarity Measures for spike trains

The aim of similarity measures is to quantify the similarity between two objects. Many similarity measures for spike trains can be categorized into the following groups: ISIs comparisons such as the bivariate ISI-distance [22], edit distances such as the Victor–Purpura distance [23] and metrics based on distances or angles between two spike train vectors as defined in (14) such as the van Rossum distance [24] and match distance [25].

2.5.1 Vector representation of spike trains

The spike train vector is defined as a weighted sum of Dirac-delta pulses

$$S_i = \sum_{m=1}^{n_i} w_i^{(m)} \delta(t - s_i^{(m)}), \tag{14}$$

where s_i denotes a spike time and n_i the total number of spiking events in spike train i. With addition defined as

$$S_i + S_j = \sum_{m=1}^{n_i} w_i^{(m)} \delta(t - s_i^{(m)}) + \sum_{p=1}^{n_j} w_j^{(p)} \delta(t - s_j^{(p)}) \tag{15}$$

and multiplication with a scalar defined as

$$aS_i = \sum_{m=1}^{n_i} a w_i^{(m)} \delta(t - s_i^{(m)}), \quad a \in \mathbb{R}, \tag{16}$$

one can show that the spike train vector satisfies the axioms for a linear vector space [25].

A advantage of the form (14) is that one can define the sample firing intensity

$$\hat{v}_X = \frac{1}{N_X} \sum_{i=1}^{N_X} S_i^{(x)}, \tag{17}$$

where N_X denotes the number of independent and identically distributed realizations of the point processes $\mathbb{S}$. It follows from the operator definitions (15) and (16) that $\hat{\boldsymbol{v}}_X$ belongs to the same vector space as the spike train S_i since the space of spike train vectors is closed under multiplication and addition.

Inner products here considered for spike train vectors can be expressed in the form

$$\langle S_i, S_j \rangle = \int_0^T \int_{-\infty}^{\infty} \int_{-\infty}^{\infty} K_\Delta \left(s, s'\right) S_i(t-s) S_j \left(t-s'\right) ds ds' dt, \tag{18}$$

where $K_\Delta(s, s')$ is a two dimensional kernel with a scalar parameter Δ. The rectangular kernel

$$K_\Delta(s, s') = \Theta(s+\Delta)\Theta(\Delta - s)\, \Theta(s'+\Delta)\Theta(\Delta - s') \tag{19}$$

and the exponential kernel

$$K_\Delta(s, s') = \Theta(s) e^{-s/\Delta}\, \Theta(s') e^{-s'/\Delta}$$

are two examples of such kernels [25].

2.5.2 Similarity measures for spike train vectors

By convention an inner product defines the norm

$$\|S_i\|^2 = \langle S_i, S_i \rangle,$$

with distance

$$D = \|\mathbf{S}_i - \mathbf{S}_j\|^2 = \langle \mathbf{S}_i - \mathbf{S}_j, \mathbf{S}_i - \mathbf{S}_j \rangle^2 = \|\mathbf{S}_i\|^2 + \|\mathbf{S}_j\|^2 - 2 \langle \mathbf{S}_i, \mathbf{S}_j \rangle \tag{20}$$

and cosine angle

$$\cos \theta_{ij} = \frac{\langle \mathbf{S}_i, \mathbf{S}_J \rangle}{\|\mathbf{S}_i\| \, \|\mathbf{S}_j\|}. \tag{21}$$

It is preferable for a similarity measure to be bounded between 0, indicating the worst possible match, and 1, indicating the best possible match. Therefore (20) is scaled and translated to construct the match distance

$$M_D(S_i, S_j) = 1 - \frac{D(S_i, S_j)}{D_{\max}} = \frac{2 \langle S_i, S_j \rangle}{\|S_i\|^2 + \|S_j\|^2}. \tag{22}$$

The cosine angle (21) may also be used as a similarity measure and is named the Pearson coefficient between two spike trains [26].

Spike trains of neural spiking events are generated from a point process. One is generally interested in comparing the firing intensity v_X of the point process generating the measured data to the firing intensity v_y of a mathematical model. A estimator for v is the sample firing rate $\hat{v}$ defined in (17) and since $\hat{v}$ belongs to the same vector space as S, the metric (22) can also be used as a similarity measure between firing rates.

It can be shown [25] that $\hat{v}$ as an estimator for v has the bias

$$b = \mathbb{E}\left[\|\hat{v}_X\|^2\right] - \|v_x\|^2 = \frac{V_x}{N_X}, \tag{23}$$

where the deviation from the firing rate V_x can be estimated by

$$\hat{V}_X = \frac{1}{N_X - 1} \sum_{i=1}^{N_X} \left\| \mathbf{S}_i^{(x)} - \hat{v}_X \right\|^2. \tag{24}$$

By subtracting the bias of $\hat{v}$ one can construct the adjusted match distance metric

$$M_D^* = \frac{2 \langle \hat{v}_X, \hat{v}_Y \rangle}{\|\hat{v}_X\|^2 - \hat{V}_X + \|\hat{v}_Y\|^2 - \hat{V}_Y}, \tag{25}$$

and the adjusted Pearson coefficient

$$\rho^* = \frac{\langle \hat{v}_X, \hat{v}_Y \rangle}{\sqrt{(\|\hat{v}_X\|^2 + \hat{V}_X)(\|\hat{v}_y\|^2 + \hat{V}_Y)}}. \tag{26}$$

2.6 Genetic algorithms

Genetic algorithms are a subset of stochastic optimization algorithms in which a population of candidate solutions are modified with the aim to find one candidate solution which maximizes a specified fitness function. Candidate solutions are named individuals and the parameters which define the specific solutions are encoded in a chromosome. In a typical genetic algorithm a new population is constructed by selecting individuals with a high fitness value with a larger probability than individuals with a low fitness value and therefore increasing the mean fitness of the population. New individuals are also created by combining the properties of two or more individuals or randomly modifying existing individuals [16].

In order to explore the parameter search space sufficiently, operations which increase the variation in the populations are employed. Two common operations to increase variation is mutation and crossover. The mutation operator adds a small random change to the selected individual's chromosome. Crossover is the process of mixing the chromosomes of two individuals at some crossover point. Two new individuals are constructed by combining the chromosome of the first individual before the crossover point with the chromosome of the second individual after the crossover point and vice versa.

A advantage of genetic algorithms is that they only require evaluations the fitness function which is in contrast to other optimization methods which often requires evaluations of the gradient of the fitness function. Genetic algorithms are therefore suitable for optimization problems with complex fitness landscapes [27].

Genetic algorithms is an iterative algorithm and the iteration steps are called generations. The chromosomes are typically encoded either as real numbers or as binary numbers [16]. A typical outline of a genetic algorithm can be seen in Algorithm 1.

Algorithm 1: A genetic algorithm

```
r ∼ unif(0, 1);
begin
    Initialize population
    for iGeneration < nGenerations do
        for iIndividuals < nIndividuals do
            Decode chromosome
            Evaluate fitness
        end
        for iSelection < N/2 do
            Select two individuals using tournament selection [16]
            Draw r
            if r > p_crossover then
                Generate two new chromosomes using crossover
                Add chromosomes to the new population
            else
                Add chromosomes to the new population
            end
            Draw r
            if r > p_mut then
                Mutate chromosome
            end
        end
        Add most fit chromosome to the new population
    end
end
```

3 Method

The methodology used in this work is to fit the Izhikevich neuron to the QSNMC dataset using a genetic algorithm. The similarity measure selected as the primary performance metric and fitness function for the genetic algorithm is the adjusted match distance (25) between two spike train vectors.

3.1 Dataset

The QSNMC dataset [11] made available by the International Neuroinformatics Coordinating Facility (INCF) includes measurements of a pyramidal neuron stimulated at the cell body with a patch-clamp electrode. The cell can be categorized as a regular spiking neuron [10]. Time series measurements of the membrane potential as well as the input current are provided in the dataset.

The input current applied by the electrode has been generated to mimic in-vivo stimulation [10] and is shown in Figure 5 with the recorded membrane voltage. To account for the noise generated by the equipment and the stochastic behavior of neurons, thirteen measurement series using identical input current waveforms have been made available [10].

The first eighteen seconds of stimulation includes three step function input sequences as well as one sequence of random input current. The purpose of these four sequences is to activate the neuron [28]. Therefore the first eighteen seconds of input have been excluded for use in the optimization or validation of the neuron model. For the remaining 21s of recorded data 70% is used to optimize the neural model and the remaining 30% is used to validate the model. The measurements recorded in

the time interval [18, 32.7] is used to optimize the model.

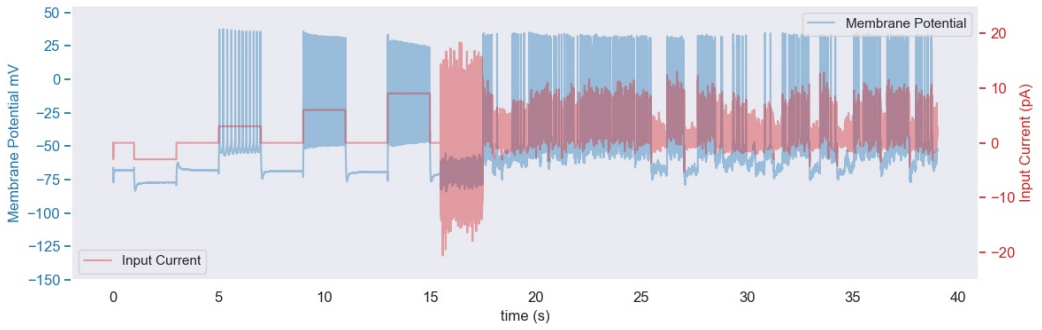

(a) The complete measurement of one measurement series.

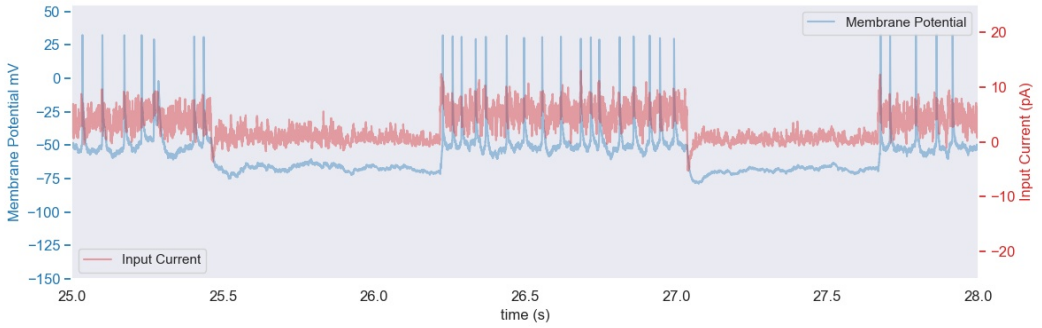

(b) Segment of the dataset.

Figure 5: Visualization of the data set. Membrane potential plotted together with the input current for one measurement series. Note that the in-vivo-like current injection starts at 18 s.

3.2 Genetic algorithm

The neural model is optimized by a genetic algorithm described in Algorithm 1. The fitness function is chosen as the adjusted match distance (25) using a rectangular kernel (19) with the scale parameter $\Delta = 2\,\text{ms}$. The scale parameter was chosen to approximate the duration of a spiking event as seen in Figure (8). The adjusted match distance compares the deterministic firing intensity of the dynamical model v_{model} with the estimator for the firing intensity of the pyramidal neuron $\hat{v}_{neuron}$ as defined in (17).

The chromosomes are encoded as real numbers initialized in $[0, 1]$. For each model parameter θ a feasibility interval $I_\theta = [a, b]$ is determined so that there exists solutions within the interval which are able to produce spiking behavior. The decoded chromosome d is generated by

$$d = a + e\,(b - a),$$

where e denotes the encoded value. No restrictions is set on e so it may leave the interval $[0, 1]$ when affected by mutation. The initial population is generated randomly by sampling uniformly from I_θ. If an individual is evaluated at fitness score 0 indicating that the model produces no spiking events then the chromosome is re-initialized from I_θ.

The chromosomes are mutated in the encoded state with mutation probability $p = \frac{1}{n_\theta}$, where n_θ denotes the number of optimization variables. The mutation operation is defined as

$$e_\theta \leftarrow e_\theta + m, \quad m \sim \mathcal{N}(0, \sigma_m), \tag{27}$$

where $\sigma_m = 0.15$. Selection is performed through tournament selection with tournament size 3 as described in [16] with tournament selection parameter $p_{\text{tour}} = 0.7$. At selection, crossover is performed with one crossover point with probability $p_{\text{crossover}} = 0.7$.

3.3 Neural model

The simplified model (2) and the extended model (3) will be fit to the INCF dataset. Furthermore, structural changes to (3) will be evaluated. The structural changes are outlined in the model

$$\begin{aligned} &C\dot{v} = k\left(v - v_{\text{r}}\right)\left(v - v_{\text{t}}\right) - u + \alpha I + f_v(u, v) \\ &\dot{u} = a\left\{b\left(v - v_{\text{r}}\right) - u\right\} + f_u(u, v) \\ &\text{if } v \geq v_{\text{peak}} \text{ , then } \begin{cases} v \leftarrow c + g_v(u, v) \\ u \leftarrow u + d + g_u(u, v) \end{cases} , \end{aligned} \tag{28}$$

where the functions $f.(u, v)$ and $g.(u, v)$ are second degree polynomials and α is scalar. Only one structural change is chosen to be non-zero at a time. Additionally, the leaky integrate-and-fire model (1) will also be fit to the dataset.

4 Results

Results for Izhikevich models fitted to the INCF dataset [11] using Algorithm (1) are summarized in Table 1. In general the models performed similarly on the validation set and the training set.

Table 1: The fitness of neuron models measured in adjusted match distance. $\deg(\cdot)$ denotes the degree of a polynomial function.

Neuron model	Training fitness	Validation fitness	Structural modification
Extended Iz.	0.9988	0.9984	α
Extended Iz.	0.9976	0.9978	$\deg(f_u(v)) = 2$
Extended Iz.	0.9964	0.9975	$\deg(f_v(u)) = 2$
LIF	0.9983	0.9972	
Simple Iz.	0.9992	0.9969	
Extended Iz.	0.9981	0.9964	
Extended Iz.	0.9961	0.9942	$\deg(g_v(u)) = 2$
Extended Iz.	0.9959	0.9927	$\deg(g_u(u)) = 2$
Extended Iz.	0.9954	0.9930	$\deg(g_u(v)) = 2$

4.1 The simple Izhikevich neuron

An optimization of the simple Izhikevich neuron (2) over 150 generations provided an optimal solution with similarity measures found in Table (1). A visualization of the simulated membrane potential for a selection of the training set and the validation set is found in Figure 7. The convergence of the optimization algorithm is visualized in Figure 6.

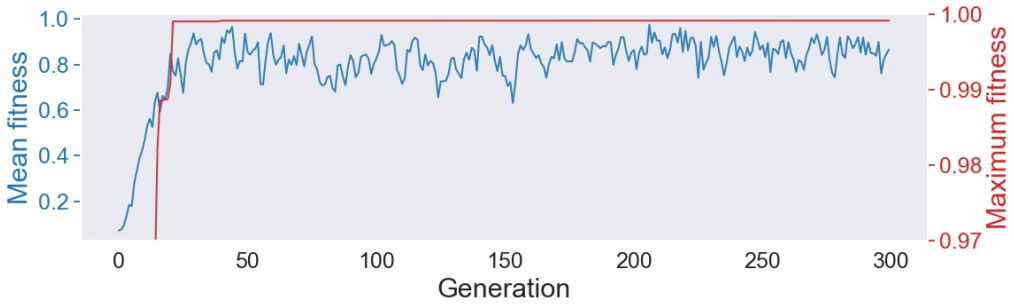

Figure 6: The maximum and mean fitness of the population during the optimization of the simple Izhikevich neuron.

4.2 The extended Izhikevich neuron

The extended Izhikevich neuron including the described structure modification was optimized over 150 generations. Table (1) describes the results for the extended Izhikevich neuron and a selection of the structure modifications. In Figure 8 the top performing extended Izhikevich neuron is visualized. The structural modification of an input resistance α to the extended Izhikevich neuron provided the model with the highest predictive strength.

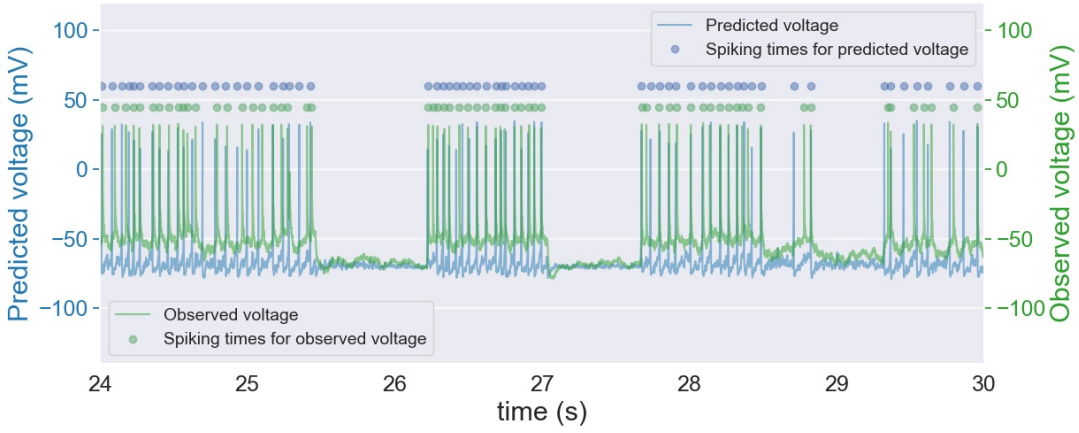

(a) Segment of the training set.

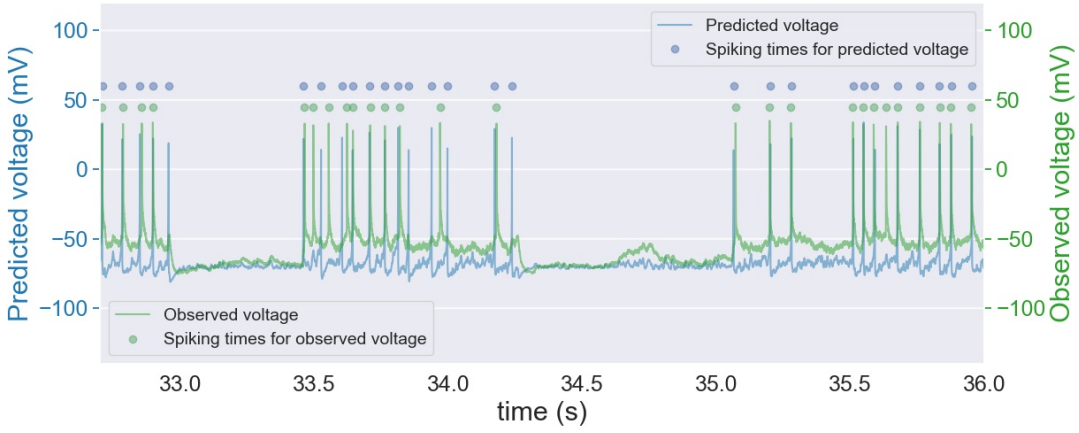

(b) Segment of the validation set.

Figure 7: Visualization of the membrane voltage predicted by the simple Izhikevich neuron. The predicted voltage exhibit significant subtreshold oscillations.

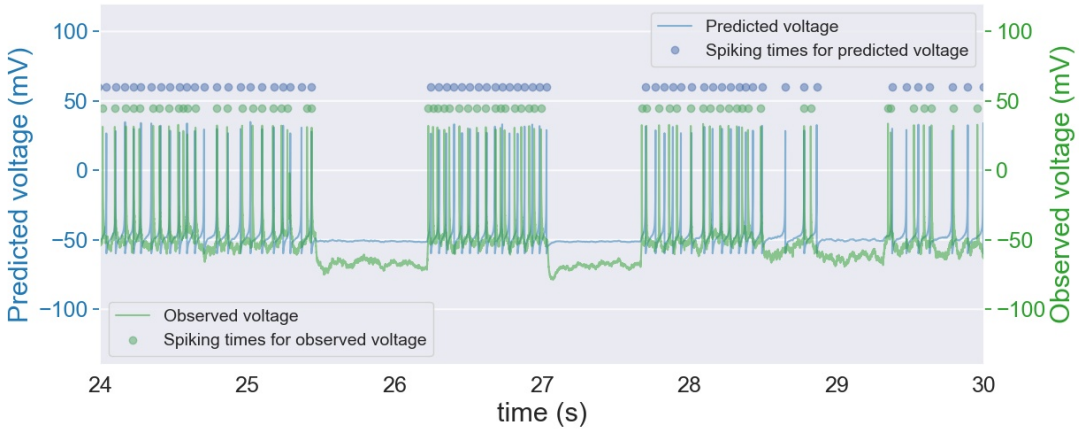

(a) Segment of the training set.

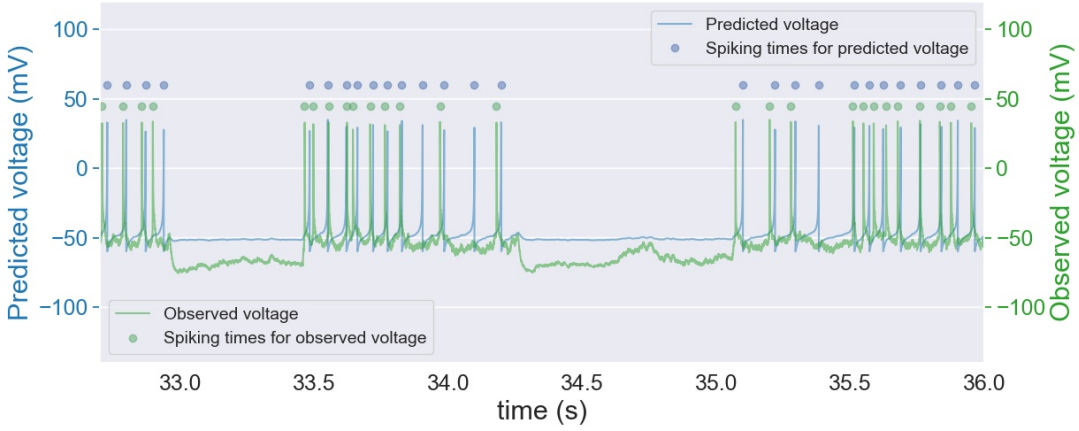

(b) Segment of the validation set.

Figure 8: Visualization of the membrane voltage predicted by the extended Izhikevich neuron with the structure modification α included as an optimization variable. The model does not exhibit subtreshold dynamics for the optimal model parameters found by the genetic algorithm.

4.3 The leaky integrate-and-fire neuron

An optimization of the leaky integrate-and-fire neuron (1) over 150 generations provided an optimal solution with fitness found in Table (1). A visualization of the simulated membrane potential for a selection of the training set and the validation set is found in Figure 9.

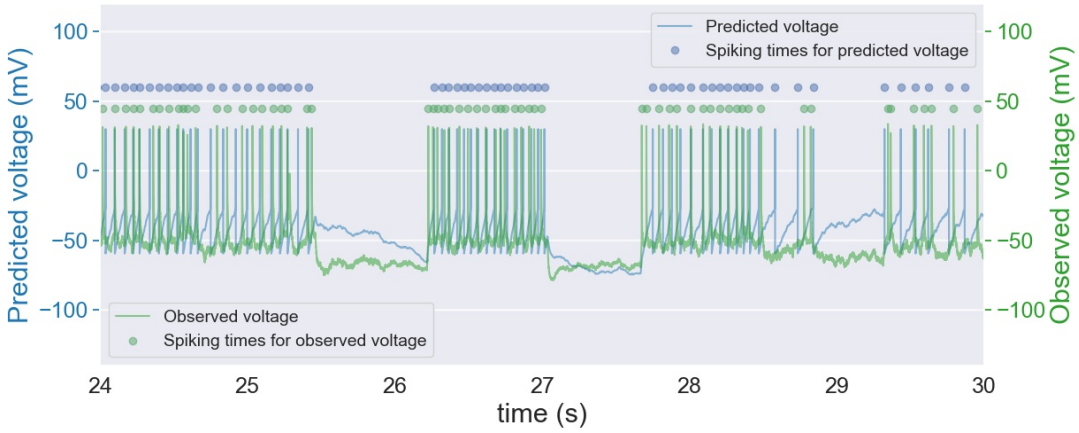

(a) Segment of the training set.

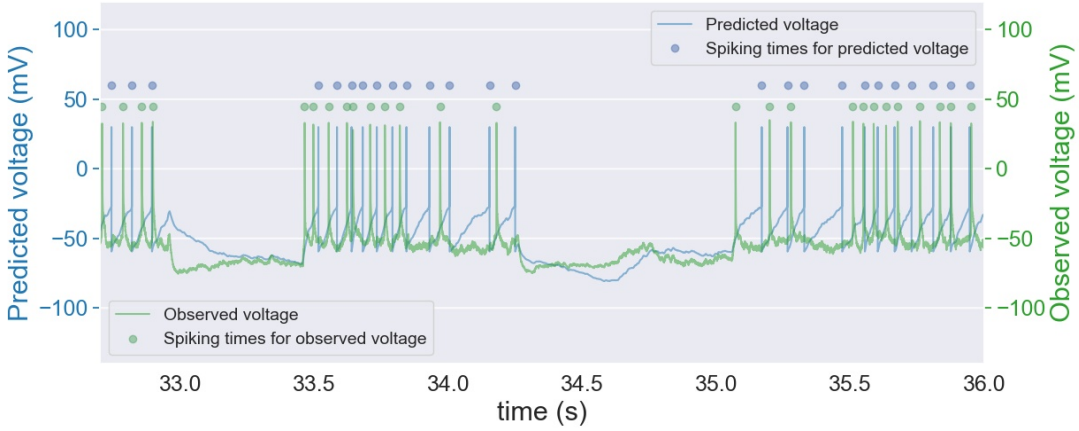

(b) Segment of the validation set.

Figure 9: Visualization of the membrane voltage predicted by the leaky integrate-and-fire model (1). Note that the profile of the predicted spike is dissimilar to the measured spiking event.

5 Discussion

In general, the models performed as well on the training set as on the validation set. The models generalize well to unseen data which may be a consequence of the models' low number of parameters.

The leaky integrate-and-fire model had performance which was close to the most predictive Izhikevich model. This indicates that the addition of a recovery variable is not helpful in modeling the spiking times of a regular spiking neuron. The unimportance of the recovery variable is corroborated by the observation that the most predictive model in Figure 8 shows almost no sub-threshold dynamics which can be compared to the second most predictive Izhikevich model shown in Figure 7 which shows sub-threshold oscillations. However, the recovery variable may provide an advantage for the Izhikevich neron when modeling neurons exhibiting bursting. Since the Izhikevich is able to produce bursting firing patterns while the LIF model can not [4].

The profile of the spiking event is not captured in the similarity metric *match distance* used in this study. However, by observing the plotted results one finds that the leaky integrate-and-fire model poorly replicates the spiking profile of the measured data. The Izhikevich model more accurately models the spiking profile.

The data used in this study was recorded with the neuron removed from its biological setting. The input current applied to the neuron attempts to mimic the input the neuron would experience in-vivo. The meaningfulness of the results in this study depend on the efficacy of the neuron when removed from other biological systems.

Structural changes with third degree polynomials are difficult to optimize using the genetic algorithm. The main difficulty was that finding a parameter interval in which there exists many solutions with non-zero fitness. The attempt using third degree polynomials achieved match distances scores significantly lower than the top performing models.

6 Conclusion

The results summarized in Table 1 show that the extended Izhikevich model with a input resistance factor included as a optimization variable produced the greatest predictive strength when fitted to the INCF dataset. Meanwhile, the simple Izhikevich model was able to fit well to the training set, achieving a match distance score of 99.92%.

The models evaluated in this study all performed well on the dataset achieving a match distance greater than 99% on the validation set. The strong performance across the models limit the number of conclusions one can draw from this work. One may speculate that the performance metric used was not able to clearly differentiate between models of varying efficacy or perhaps the dataset represents a task which is too simple to evaluate the performance of the models.

6.1 Future work

An optimization run of the Izhikevich took between 12 - 24 hours depending on number of generations and the population size. The runtime of the optimization may be prohibitively large to sufficiently explore the possible neuron models as well as the parameter intervals. Therefore it may be beneficial to use a CPU parallelization framework such as OpenMP or GPU acceleration through frameworks such as OpenCL or CUDA.

References

[1] Alan L Hodgkin and Andrew F Huxley. A quantitative description of membrane current and its application to conduction and excitation in nerve. *The Journal of physiology*, 117(4):500–544, 1952.

[2] Eugene M. Izhikevich. Which model to use for cortical spiking neurons? *IEEE Transactions on Neural Networks, VOL. 15, NO. 5*, 2004.

[3] Aleksei Dmitrichev, Dmitry Kasatkin, Vladimir Klinshov, Sergey Kirillov, Oleg Maslennikov, D.S. Shchapin, and Vladimir Nekorkin. Nonlinear dynamical models of neurons: Review. *Izvestiya Vysshikh Uchebnykh Zavedeniy. Prikladnaya Nelineynaya Dinamika*, 26:5–58, 01 2018.

[4] Eugene M. Izhikevich. Simple model of spiking neurons. *IEEE Transactions on Neural Networks, VOL. 14, NO. 6*, 2003.

[5] Tomoyuki Kubota, Kohei Nakajima, and Hirokazu Takahashi. Information processing using a single izhikevich neuron. pages 550–557, 01 2018.

[6] Gautam Kumar, Vikram Aggarwal, Nitish Thakor, Marc Schieber, and Mayuresh Kothare. Design and control of a closed-loop neural prosthesis. 11 2010.

[7] Zachary F Mainen and Terrence J Sejnowski. Influence of dendritic structure on firing pattern in model neocortical neurons. *Nature*, 382(6589):363–366, 1996.

[8] Thomas Heiberg, Birgit Kriener, Tom Tetzlaff, Gaute T Einevoll, and Hans E Plesser. Firing-rate models for neurons with a broad repertoire of spiking behaviors. *Journal of computational neuroscience*, 45(2):103–132, 2018.

[9] Renaud Jolivet, Felix Schürmann, Thomas K Berger, Richard Naud, Wulfram Gerstner, and Arnd Roth. The quantitative single-neuron modeling competition. *Biological cybernetics*, 99(4-5):417, 2008.

[10] Wulfram Gerstner. How good are neuron models? *Science, vol. 326, Issue 5951*, 2009. `https://science-sciencemag-org.proxy.lib.chalmers.se/content/326/5951/379`.

[11] INCF. *Dataset: Quantitative Single Neuron Modeling Competition*, accessed: 01.06.2020. `https://github.com/INCF/QSNMC`.

[12] Eoin P Lynch and Conor J Houghton. Parameter estimation of neuron models using in-vitro and in-vivo electrophysiological data. *Frontiers in neuroinformatics*, 9:10, 2015.

[13] Cyrille Rossant, Dan FM Goodman, Bertrand Fontaine, Jonathan Platkiewicz, Anna K Magnusson, and Romain Brette. Fitting neuron models to spike trains. *Frontiers in neuroscience*, 5:9, 2011.

[14] Sahar Hojjatinia, Mahdi Aliyari Shoorehdeli, Zahra Fatahi, Zeinab Hojjatinia, and Abbas Haghparast. Improving the izhikevich model based on rat basolateral amygdala and hippocampus neurons, and recognizing their possible firing patterns. *Basic and Clinical Neuroscience*, 11(1):79, 2020.

[15] Gautam Kumar, Vikram Aggarwal, Nitish V Thakor, Marc H Schieber, and Mayuresh V Kothare. Optimal parameter estimation of the izhikevich single neuron model using experimental inter-spike interval (isi) data. In *Proceedings of the 2010 American Control Conference*, pages 3586–3591. IEEE, 2010.

[16] Mattias Wahde. *Biologically inspired optimization methods: an introduction*. WIT press, 2008.

[17] Hartmut Logemann and Eugene P Ryan. *Theorem 2.5, Ordinary differential equations*, pages "28–29". Springer, 2014.

[18] W. Gerstner and W Kistler. *Spiking Neuron Models: Single Neurons, Populations, Plasticity*. Cambridge University Press, 2002.

[19] Moshe Abeles. Time is precious. *Science*, 304(5670):523–524, 2004.

[20] Eugene M Izhikevich. *Dynamical systems in neuroscience*. MIT press, 2007.

[21] VI Krinskii and Yu M Kokoz. Analysis of equations of excitable membranes-i. reduction of the hodgkin-huxley equations to a second order system. *Biophysics*, 18(3):533–539, 1973.

[22] Thomas Kreuz, Daniel Chicharro, Ralph G Andrzejak, Julie S Haas, and Henry DI Abarbanel. Measuring multiple spike train synchrony. *Journal of neuroscience methods*, 183(2):287–299, 2009.

[23] Jonathan D Victor and Keith P Purpura. Nature and precision of temporal coding in visual cortex: a metric-space analysis. *Journal of neurophysiology*, 76(2):1310–1326, 1996.

[24] MCW van Rossum. A novel spike distance. *Neural computation*, 13(4):751–763, 2001.

[25] Richard Naud. Improved similarity measures for small sets of spike trains. *Neural Computation 23(12):3016-69*, 2011.

[26] JJ Eggermont, AMHJ Aertsen, and PIM Johannesma. Quantitative characterisation procedure for auditory neurons based on the spectro-temporal receptive field. *Hearing research*, 10(2):167–190, 1983.

[27] Terry Jones et al. *Evolutionary algorithms, fitness landscapes and search*. PhD thesis, Citeseer, 1995.

[28] INCF. *Quantitative Single-Neuron Modeling: Competition 2009 Description*, 2009 (accessed January 25, 2020). `https://pdfs.semanticscholar.org/cb2c/7a2ff006349e763b08d7067de00f0308657d.pdf`.